XL CILAMCE
IBERO-LATIN AMERICAN CONGRESS ON COMPUTATIONAL METHODS IN ENGINEERING
NOVEMBER 11-14, 2019
Praiamar Natal Hotel & Convention
Natal, RN-BRAZIL

# SELF-SUPPORTING LATTICE TOWER UNDER DYNAMIC WIND LOADS

**Claudia Slongo**
**Marcos Arndt**
*claudiaslongo@ufpr.br*
*arndt@ufpr.br*
*Federal University of Paraná*
*Av. Cal. Francisco H dos Santos, 100, 81530-000, Paraná, Brazil*

**Abstract.** The difficulty to determine time-variant loadings, such as wind loading, stands out among the structural engineering challenges. For example, the wind is the preponderant action in a self-supporting lattice tower, and its wrong estimation can lead to unwanted vibration and displacements in the structure. Those structures are usually designed with a simplified dynamic effect, in which the wind is considered as a static load, increasing its value by dynamic coefficients proposed in standard codes. However, this simplification can easily lead an improper design. Although there are various non-standard methods for the determination of the time variant loading of the wind in order to achieve a more accurate and reliable analysis, this work focuses on the Synthetic Wind Method, that is a non-deterministic process using the Monte Carlo simulation in order to obtain wind loadings by superposition of harmonic functions with random phase angles. This work provides a dynamic analysis of a self-supporting lattice tower using the Synthetic Wind Method with different wind spectra (Davenport, slightly modified Davenport, Harris and Kaimal). A comparison between the dynamic and the static response obtained by the Brazilian code NBR 6123/1988 – Forces due to wind on buildings is also made. The structure calculated with the original and the slightly modified Davenport spectra have given similar and the largest displacement responses. Whereas the Harris power spectral density proved to be the least conservative for this study.

**Keywords:** Dynamic response, Synthetic Wind Method, Self-supporting lattice tower

# 1 Introduction

Natural phenomena are intrinsically dynamic, i.e, their loads vary according to time. Wind loads are not different; they have not only dynamic properties but also have random characteristics. That's why one of the greatest challenges in structural engineering is the determination and simulation of the wind loading. The dynamic structural responses related to wind are normally higher for light and tall constructions, in which the wind can trigger instabilities and may be the main influence for the structural design (e.g. telecommunication towers, membranes and cables). The negligence of the dynamic effects in telecommunication towers can lead to excessive deformations not foreseen in the static analysis, which can affect the signal transmission of the antennas.

The wind loading's dynamic effects are usually considered only by the increase of the static effect by appropriate coefficients. The Brazilian standard NBR 6123/1988 – Forces due to the wind in buildings [1] – establishes three procedures to calculate wind loadings in structures. They are: the method of statically equivalent loads, the simplified method and the discrete method. Although the simplified and the discrete methods have dynamic characteristics, they not generate dynamics loads, but statics loads that are dependent of the fundamental frequency and of the vibration period of the structure.

In order to obtain realistic dynamic forces in structures under wind loading, engineers make use of non-standard methods. A known Brazilian non-standard method is the Synthetic Wind Method developed by Franco [2]. This Brazilian method determines the fluctuating (or dynamic) pressure of the wind and simulates its load over time. With the aid of a wind spectral density, usually the Davenport one, and the Monte Carlo numerical technique, the Franco's procedure is based on the sum of harmonics of several frequencies, with randomly angle phases, in order to simulate the fluctuating portion of the wind speed.

The main objective of this work is to provide a dynamic analysis of a self-supporting lattice telecommunication tower using the Synthetic Wind Method adopting different spectra of the wind (Davenport, slightly modified Davenport, Harris and Kaimal). Besides, a comparison between the dynamic responses and the static response obtained by the Brazilian code NBR6123/1988 – Forces due to wind on buildings - is also made.

# 2 Dynamic Action of the Wind in Structures

Due to the randomness of their variation, wind properties are statistically treated [3]. The average wind speed *U* can be considered a stochastic variable, which can be estimated by a long period of time analysis (usually between ten minutes and one hour), while the fluctuating wind speed component *u(t)* is based on short term statistics (usually between three and five seconds). The sum of the average wind speed with the gusting effect is the resulting wind load. These two variables are analyzed separately, and the total effect is a result of overlapping effects given by:

$$U_{Total} = U + u(t). \tag{1}$$

Because of its stochastic property, the variation of the wind speed over time produces a Gaussian distribution [4] as illustrated in Fig. 1. To define the fluctuating portion of the wind speed *u(t)*, it is necessary to know the concept of power spectrum.

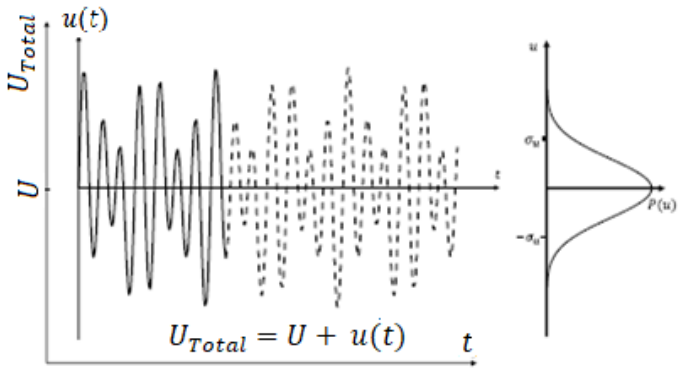


Figure 1. Wind speed variation and its Gaussian distribution [4]

## 2.1 Wind-spectral density

Wind gusts are random and there are no discrete frequencies at which gusts occur [5]. However, there is a considerable amount of energy concentrated at frequencies whose periods correspond between 1 second and 5 minutes (Fig. 2). Such wind energy can be described by a power spectrum density.

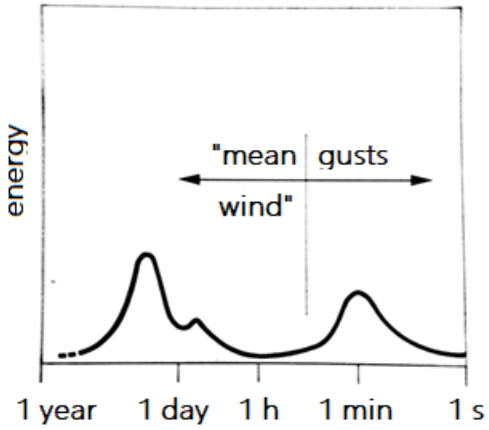


Figure 2. Wind energy distribution according to its period

The wind power $W$, within a certain period of time and at a certain height, can be calculated as:

$$dW = S(n)dn. \tag{2}$$

where $n$ is the frequency of the wind gust and $S(n)$ is the power spectral density of the wind speed.

The power spectral density of a random phenomenon determines a measure of the energy distribution of the harmonic velocity present in various frequencies [6]. Therefore, it is fundamental to calculate dynamic responses for structures under wind loading.

A generic mathematical expression of power spectral density is described by:

$$\frac{n\,S}{{u_*}^2\,\phi_e^{2/3}} = \frac{A\,x}{(1+Bx)^{2/3}}. \tag{3}$$

$$x = \frac{n\,z}{U0}. \tag{4}$$

where *S* is the wind power spectral density, *A* and *B* are empirical coefficients, $\phi_e$ is the turbulent kinetic energy dissipation rate, *x* is the dimensionless frequency, *n* is the gust frequency, $U0$ is the average wind speed at 10 meters high during 10 minutes and $u_*$ is the shear wind velocity

One of the most commonly used spectra in structural engineering is the power spectral density suggested by Davenport that is given by:

$$S(n) = 4\,\frac{x(n)^2\ {u_*}^2}{n\,[1\ + x(n)^2]^{4/3}}. \tag{5}$$

$$x(n) = \frac{1200\,n}{U0}. \tag{6}$$

The average wind speed at 10 meters high and during 10 minutes (*U0*) can be calculated as a function of the basic wind speed *V0* [6][8] as determinated by:

$$U0 = 0{,}69\,V0. \tag{7}$$

The shear wind velocity can be expressed by:

$$u_* = \frac{U0}{2{,}5\,ln\left(\frac{10}{z0}\right)}. \tag{8}$$

where *z0* is roughness length for various types of terrain.

In "Direct along-wind dynamics analysis of tall structures" [2], Franco used the slightly modified Davenport spectrum, which is adopted by the National Building Code of Canada, to calculate the fluctuating pressures of the wind for a practical example using the Synthetic Wind Method. The slightly modified Davenport spectrum is given by:

$$S(n) = 4\,\frac{x(n)^2\ {u_*}^2}{n\,[1\ + x(n)^2]^{4/3}}. \tag{9}$$

$$x(n) = \frac{1220\,n}{U0}. \tag{10}$$

According to Franco [2], by using a logarithmic representation scale, the power spectral density function can be conveniently described in its reduced form $Sp(n)$. The reduced spectrum was previously studied by Davenport [9] and Kaimal et al. [10], who found an expression for wind speed longitudinal fluctuations without the significant influence of local characteristics. The reduced form of the power spectral density is given by:

$$Sp(n)\ d(log_e n) = \frac{n\,S(n)}{{u_*}^2}\,\frac{1}{n}\,dn = \frac{dW}{{u_*}^2}. \tag{11}$$

i.e.:

$$Sp(n) = \frac{n\,S(n)}{u_*^2}. \tag{12}$$

Although the Davenport power spectrum is best suited for standards such as the American National Standards Institute and National Building Code of Canada, it cannot adequately represent low frequency values and does not consider the influence of the structure height [11]. Besides the

Davenport's original and slighted modified spectra, there are others that are well known in the literature such as the Kaimal, Harris and the von Kármán power spectral densities.

In Fig. 3, the abscissa axis represents the number of waves in cycles per meter, $f/V$, in which $\bar{V}(z)$ is the mean hourly speed at the height $z$ and $f$ is the frequency of the gust in Hz. In the ordinate axis the power spectral density is normalized by the variance ($\sigma^2$). Thus the area under the curve between two frequencies is proportional to the total energy [11]. The main differences between Harris, Davenport and von Kármán spectra are due to the lack of resemblance in the scale length used in the formulations [9].

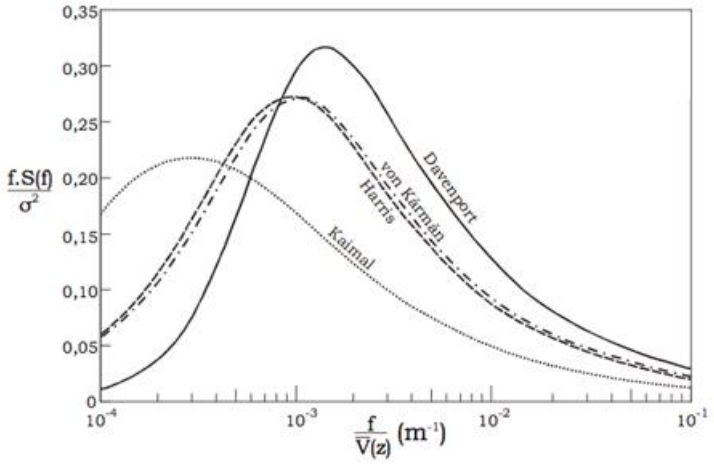


Figure 3. Davenport, Harris, von Kármán and Kaimal wind spectral densities

Harris modified the formulation proposed by Davenport [12], reaching the following spectrum:

$$S(n) = 4\,\frac{x(n)^2\ {u_*}^2}{n\,[2\ + x(n)^2]^{5/6}}. \tag{13}$$

$$x(n) = \frac{1800\,n}{U0}. \tag{14}$$

Kaimal et al. [10] suggested the following power spectral density formulation that takes the structure's height $z$ into account:

$$S(n,z) = \frac{200\ {u_*}^2\,x(z,n)}{n\,[1 + 50\,x(z,n)]^{5/3}}. \tag{15}$$

$$x(z,n) = \frac{z\,n}{U(z)}. \tag{16}$$

## 3 The Synthetic Wind Method

The Synthetic Wind Method, developed by Franco [2], can be considered similar to a Monte Carlo simulation because it generates a reasonably large number of load series composed by the superposition of randomly chosen phase harmonic components. According to his method, the wind speed is decomposed in two parts: the dynamic part, or fluctuation one, and the static part. Franco made this division based on the Brazilian wind standard NBR 6123/1988 that defines values for the peak velocity measured in short time intervals (2 to 5 seconds). With values for the peak velocity, it is possible to determine the mean velocities, which are measured in a time interval of minimum 10

minutes. Based on the ratio between instantaneous peak pressure (measured in 3 seconds) and mean pressure (measured in 600 seconds) given by the Brazilian standard, it is feasible to calculate the percentages of mean and fluctuating pressure in the form:

$$\frac{p_{600}}{p_3} = \left(\frac{U_{600}}{U_3}\right) = 0{,}69^2 = 0{,}48. \tag{17}$$

Therefore, the Synthetic Wind Method determines that 48% of the total pressure of the wind is static and the remaining 52% represents gust. The dynamic loads are generated through a wind power spectrum and it is decomposed into a finite number of harmonic functions that varies from 0 to 600 s and are proportional (usually multiple of 2) to the resonant frequency of the structure. The number of harmonics must be greater than or equal to eleven and one of these harmonics must be the resonant one. The greater the number of functions, the more accurate the method is.

The random characteristic of the dynamic load is given by the use of arbitrarily generated phase angles in the method. Furthermore, appropriate transformations (such as Fourier's) are required to calculate the fluctuating pressures, or dynamic pressures, of the wind.

The procedure is terminated when the structure is excited by a function composed of the successive sum of the randomly combined harmonics, thereby generating a determined number of samples to calculate the characteristic response.

The dynamic parcel of the wind loading is applied as the fluctuating pressure where transformed into equivalent gusts, i.e, such loading is performed over a gust duration and at an unfavorable part of the structure. With the spatial correlational functions proposed in Synthetic Wind Method, the dynamic wind loading is simulated at various parts of the structure with maximum amplitudes.

### 3.1 Decomposition of the fluctuating pressures

The fluctuating pressures *p'(t)*, equivalent to 52% of the total wind pressure, is a random, stationary, ergodic, gaussian process of zero mean and can be written through a Fourier series:

$$p'(t) = \sum_{k=1}^{m} C_k \cos\left(\frac{2\,\pi}{T_r\, r_k} t - \theta_k\right). \tag{18}$$

In the Equation (18), *m* is the number of harmonics (that must be greater than or equal to eleven), $T_r$ is the structure fundamental period, $\theta_k$ is the randomly generated phase angle (within a range of 0 to 2 π) and $r_k$ is a relation between the harmonics *k* and *r*:

$$r_k = 2^{k-r}. \tag{19}$$

where *k* is the harmonic in evidence and *r* is the resonant harmonic.

The factor $C_k$ is calculated by the integration of the power spectral density over the *m* harmonic frequency ranges:

$$C_k = \sqrt{\int_k 2\, Sp(f)\, d(f)}. \tag{20}$$

Since the maximum pressure amplitude can be writtem as a portion of the total pressure, the values of $C_k$ can be "corrected" by the coefficients $c_k$, obtained by:

$$c_k = \frac{C_k}{\sum_1^m C_k}. \tag{21}$$

Franco [2] also suggests making one more correction of the $c_k$ coefficient but only for the values of $k = r$ (resonant) and its adjacent harmonics ($k = r + 1$ and $k = r - 1$):

$$c_r' = \frac{c_r}{2}. \tag{22}$$

$$c_{r-1}' = c_{r-1} + \frac{c_r}{4}. \tag{23}$$

$$c_{r+1}' = c_{r+1} + \frac{c_r}{4}. \tag{24}$$

With the corrected coeficientes, the Eq. (18) can be written as:

$$p''(t,k) = \sum_{k=1}^{m} c_k \cos\left(\frac{2\pi}{T_r r_k} t - \theta_k\right). \tag{25}$$

### 3.2 Spatial correlations of velocities and pressures fluctuations

The spatial correlation allows the study of the non-uniformity of the gust actions along the structures. The measure of the spatial correlation is the narrow band cross correlation coefficient *Coh(dist,f)*, that is a function of the gust frequency and the distance between two point (*dist*):

$$Coh\,(dist, f) = e^{-\hat{f}}. \tag{26}$$

with:

$$\hat{f} = \frac{f\sqrt{C_z^2\,(z_2 - z_1)^2 + C_y^2\,(y_2 - y_1)^2}}{U0}. \tag{27}$$

where *z* and *y* are the coordinates for two points $(x_1, y_1, z_1)$ and $(x_2, y_2, z_2)$ of the face of the structure exposed to the wind with same horizontal coordinate *x*. The terms $C_z$ and $C_y$ are obtained experimentally and, for practical applications, the values $7 \leq C_z \leq 10$ and $12 \leq C_y \leq 16$ can be adopted [2]. On the side of safety, the values $C_z$ = 7 and $C_y$ = 12 are adopted. Besides, in predominantly vertical structures and for slender buildings it is suffices to consider only the vertical correlation.

Therefore, Eq. 26 can be written as (with $z_2 - z_1 = dist = \Delta z$):

$$Coh\,(\Delta z, f) = exp\left(-\frac{7\,\Delta z\, f}{V_0}\right). \tag{28}$$

From the Eq. 28 above, it is remarkable that the correlation coefficient ranges from 1 ($\Delta z = 0$) to zero ($\Delta z \to \infty$). This linear function behavior provides the concept of the "gust size" ($\Delta z$), i.e, the size of a perfectly correlated gust that induces the same effect on the structure (Fig. 4) given by:

$$\Delta z = \frac{U0}{7\,f}. \tag{29}$$

$$2\,\Delta z = \frac{2U0}{7\,f}. \tag{30}$$

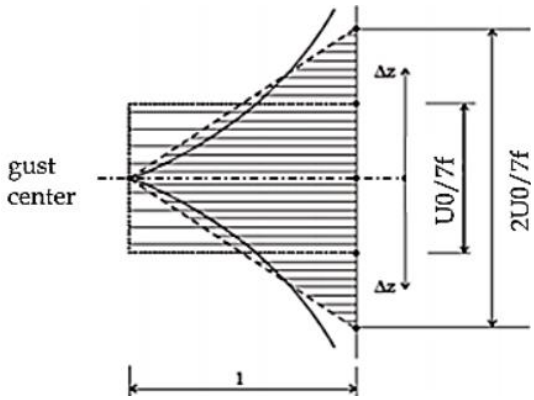


Figure 4. Equivalent gusts

According to Franco [2], it is necessary to define de gust center deterministically, which can be done by assuming that the gusts are stationary and calculating, for each of the *m* harmonics, the position that maximizes the relevant response of the structure. Nonetheless, it is suffices to suppose that all the elementary gusts have the same center. A simple expression is proposed to analytically determine the gust center ($G_c$), where $z_1$ is the highest point of the structure [13], given by:

$$G_c = z_1 - \Delta z. \tag{31}$$

Adopting the gust center $G_c$, the coefficients of reduction of the fluctuating pressures $Cr$, which vary with the height $z_j$ and the harmonic *k* can be written as:

$$Cr = \left(\frac{1}{\Delta z}\right)\left(G_c - z_j\right) + 1 \text{ if } G_c \leq z_j \leq G_c + \Delta z. \tag{32}$$

or,

$$Cr = \left(\frac{-1}{\Delta z}\right)\left(G_c - z_j\right) + 1 \text{ if } G_c - \Delta z \leq z_j \leq G_c. \tag{33}$$

otherwise,

$$Cr = 0. \tag{34}$$

## 4 Analytical Model

The research object is a self-supporting telecommunication tower. It is 30 meters high and has an equilateral triangle cross section. The tower has three platforms and an antenna at the top (Fig. 5).

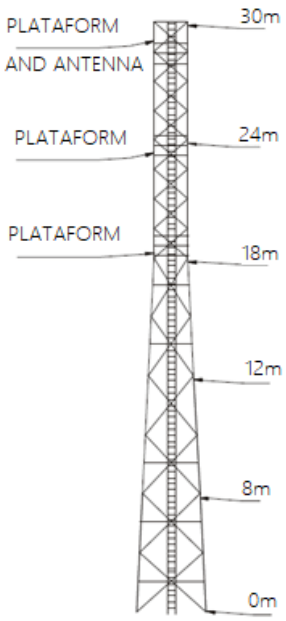


Figure 5. The telecommunication tower

The tower was analyzed with the software ANSYS using spatial lattice finite elements. The platforms and the antenna were idealized as concentrated mass elements. The base of the structure was considered totally fixed (U1=U2=U3=R1=R2=R3=0). The vertical members of the tower are of high mechanical strength steel (yield limit of 373 MPa) and have a tube section profile. The diagonal and horizontal members of the tower are of ASTM A36 (yield limit of 250 MPa) and have an L-Section profile. The telecommunication tower was modeled for a hypothetical region at south of Brazil. Furthermore, it was considered that total or partial ruin could affect the safety or the possibility of rescuing people after a destructive storm. Therefore, the considered parameters of NBR 6123/1988 are listed at Table 1.

As stated in the Brazilian standard, the basic wind speed (*V0*) is the average speed over 3 seconds for a recurrence period of 50 years, at a height of 10 meters above the ground at an open and flat land. As a general rule, it is assumed that the base wind can blow from any horizontal direction.

Table 1. Project parameters

| | |
|---|---|
| Operating Wind | 100 km/h |
| Basic wind speed (V0) | 45 m/s (South Brazil) |
| S1 (terrain topographic coefficient) | 1,10 (non-flat ground surface) |
| S3 (statistical coefficient) | 1,10 (the ruin could affect the possibility of rescuing people) |
| Terrain roughness | IV Category |
| “Edification Class” | Class B |

The performed dynamic analysis did not take into account the nonlinear behavior of the structure. Moreover, the modeled wind loading has been simplified as unidirectional, stationary and homogeneous.

The telecommunication tower was separated into five modules (Fig. 6). For each module was calculated the equivalent area, drag coefficient, the static and fluctuating pressures. Both dynamic and static forces were applied at the top of each module. Besides the wind action, the weight of the antenna, platforms, stairs and cables were also considered. The dead loads for each module are listed in the following table (Table 2). The live loads of assembly were disregarded because the maximum wind loading is unlikely to occur exactly during the tower installation or maintenance.

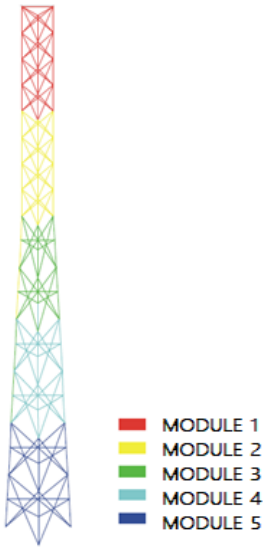


Figure 6. The five modules of the tower

Table 2. Dead loads

| Module | Structure weight (N) | Stairs and cables weight (N) | Platforms weight (N) | Antenna weight (N) | Total weight (N) |
|---|---|---|---|---|---|
| 1 | 1898,99 | 1560,00 | 600,00 | 3000,00 | 7058,99 |
| 2 | 1898,99 | 1560,00 | 120,00 | - | 4658,99 |
| 3 | 2573,09 | 1560,00 | - | - | 4122,09 |
| 4 | 2961,48 | 1560,00 | - | - | 4521,48 |
| 5 | 4014,65 | 1560,00 | - | - | 5574,65 |
| Total | | | | 25936,20 | |

The characteristic velocity (*Vk*) for each module was calculated as stated in the NBR 6123/1988 by:

$$Vk = V0\ S1\ S2\ S3. \tag{35}$$

where *S2* is a coefficient that varies with the module height (*z*), gust factor (*Fr*), meteorological factor (*b*) and the coefficient (*p*) given by:

$$S2 = b\ Fr\ \left(\frac{z}{10}\right)^{p}. \tag{36}$$

The *S2* factors and the characteristic velocity for each tower module are listed in Tables 3 and 4 respectively.

Table 3. S2 factor

| Module | Fr | b | p | z (m) | S2 |
|---|---|---|---|---|---|
| 1 | 0,98 | 0,85 | 0,125 | 30,00 | 0,9556 |
| 2 | 0,98 | 0,85 | 0,125 | 24,00 | 0,9293 |
| 3 | 0,98 | 0,85 | 0,125 | 18,00 | 0,8965 |
| 4 | 0,98 | 0,85 | 0,125 | 12,00 | 0,8522 |
| 5 | 0,98 | 0,85 | 0,125 | 6,00 | 0,7815 |
| Antenna | 0,98 | 0,85 | 0,125 | 30,00 | 0,9556 |
| Platform | 0,98 | 0,85 | 0,125 | 30,00 | 0,9556 |
| Platform | 0,98 | 0,85 | 0,125 | 25,00 | 0,9341 |
| Platform | 0,98 | 0,85 | 0,125 | 18,00 | 0,8965 |

Table 4. Characteristic velocity (Vk) for each module

| Module | V0 (m/s) | S1 | S2 | S3 | Vk (m/s) |
|---|---|---|---|---|---|
| 1 | 45,00 | 1,10 | 0,9556 | 1,10 | 52,03 |
| 2 | 45,00 | 1,10 | 0,9293 | 1,10 | 50,60 |
| 3 | 45,00 | 1,10 | 0,8965 | 1,10 | 48,81 |
| 4 | 45,00 | 1,10 | 0,8522 | 1,10 | 46,40 |
| 5 | 45,00 | 1,10 | 0,7815 | 1,10 | 42,55 |
| Antenna | 45,00 | 1,10 | 0,9556 | 1,10 | 52,03 |
| Platform | 45,00 | 1,10 | 0,9556 | 1,10 | 52,03 |
| Platform | 45,00 | 1,10 | 0,9341 | 1,10 | 50,86 |
| Platform | 45,00 | 1,10 | 0,8965 | 1,10 | 48,81 |

For the drag coefficient estimation (*Ca*), the exposed area index and the number of Reynolds for each tower module were calculated. For the antenna and platforms, the drag coefficient equal to 1,60 was adopted (Table 5).

Table 5. Drag Coefficient

| Module | Ca |
|---|---|
| 1 | 1,565 |
| 2 | 1,565 |
| 3 | 1,592 |
| 4 | 1,663 |
| 5 | 1,712 |
| Antenna | 1,600 |
| Platform | 1,600 |
| Platform | 1,600 |
| Platform | 1,600 |

### 4.1 Modal analysis

Before the application of the Synthetic Wind Method, a modal analysis was performed on the self-supporting tower. Using the consistent mass matrix and with the aid of ANSYS software, the Table 6 shows the first ten frequencies of the structure. The Figures 7, 8 and 9 illustrate the first three modes of the tower vibration.

Table 6. Frequencies and natural periods of the structure

| Vibration Mode | Natural Frequency (Hz) | Period (s) |
|---|---|---|
| 1 | 1,255 | 0,797 |
| 2 | 1,256 | 0,796 |
| 3 | 6,080 | 0,164 |
| 4 | 6,152 | 0,163 |
| 5 | 8,918 | 0,112 |
| 6 | 15,989 | 0,063 |
| 7 | 16,238 | 0,062 |
| 8 | 16,743 | 0,060 |
| 9 | 22,977 | 0,044 |
| 10 | 25,195 | 0,040 |

Analyzing Table 6 and the Fig. 7 and 8, it is notable that the first two frequencies are similar, as their modes. The first natural frequency was used as the resonant harmonic for the application of the Synthetic Wind Method.

Figure 7. First vibration mode

Figure 8. Second vibration mode

Figure 9. Third vibration mode

### 4.2 Static Wind Loading Component

As previously described, the Synthetic Wind Method is composed of two components: the static wind loading (that represent 48% of the total pressure) and the gusts (or dynamic pressures, that are the remaining 52%). The calculation of the static wind forces (*Fm*) shown in Table 7, the meteorological coefficient $b$ and p at the interval of 3s and 600s ($b_3 = 0{,}86, p_3 = 0{,}12$, $b_{600} = 0{,}71$ and $p_{600} = 0{,}23$), the peak pressure ($q_3$), the static pressure ($q_{600}$) and the dynamic pressure ($q_f$) were estimated according the NBR 6123/1988. The pressures (peak, static and dynamic) are obtained by:

$$q_3 = 0{,}613\ v_3^2. \tag{37}$$

$$q_{600} = 0{,}613\ v_{600}^2. \tag{38}$$

$$q_f = q_3 - q_{600}. \tag{39}$$

Table 7. Static, peak and dynamic pressures and the static wind forces

| Module | z (m) | Effective Area (m²) | Ca | V0 (m/s) | v3 (m/s) | v600 (m/s) | $q_3$ (N/m²) | $q_f$ (N/m²) | $q_{600}$ (N/m²) | **Fm (N)** |
|---|---|---|---|---|---|---|---|---|---|---|
| 1 | 30,00 | 3,94 | 1,57 | 45,00 | 44,15 | 28,38 | 1195,06 | 701,24 | 493,83 | **3045,00** |
| 2 | 24,00 | 3,94 | 1,57 | 45,00 | 42,99 | 26,96 | 1132,75 | 687,09 | 445,65 | **2747,95** |
| 3 | 18,00 | 4,40 | 1,59 | 45,00 | 41,53 | 25,24 | 1057,18 | 666,76 | 390,41 | **2734,77** |
| 4 | 12,00 | 4,78 | 1,66 | 45,00 | 39,56 | 22,99 | 959,15 | 635,16 | 323,98 | **2575,40** |
| 5 | 6,00 | 5,49 | 1,71 | 45,00 | 36,40 | 19,60 | 812,15 | 576,62 | 235,53 | **2213,74** |
| Antenna | 30,00 | 4,08 | 1,60 | 45,00 | 44,15 | 28,38 | 1195,06 | 701,24 | 493,83 | **3223,71** |
| Platform | 30,00 | 0,30 | 1,60 | 45,00 | 44,15 | 28,38 | 1195,06 | 701,24 | 493,83 | **237,04** |
| Platform | 25,00 | 0,30 | 1,60 | 45,00 | 43,20 | 27,22 | 1143,90 | 689.80 | 454,10 | **217,97** |
| Platform | 18,00 | 0,30 | 1,60 | 45,00 | 41,53 | 25,24 | 1057,18 | 666,76 | 390,41 | **187,40** |

Among the cases of wind incidence on the structure, only one was analyzed and it is represented in Fig. 10. The distribution of the wind loads of each node (1, 2 and 3) was also made according to the NBR 6123/1988

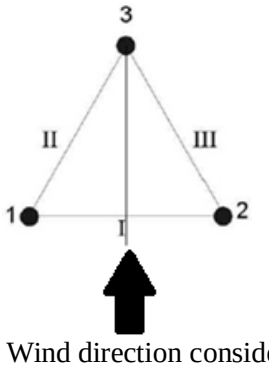


Figure 10. Wind direction considered

### 4.3 Dynamic Wind Loading Component

As stated in Franco [2], a spectrum of eleven harmonics (Table 8) ranging from 0 to 600 s, that were made of multiple of two from the natural period of the structure, were developed. The harmonic number 3 (*k=3*) correspond to the fundamental frequency of the tower.

Table 8. Spectrum of Harmonics

| k | Period T (s) | Frequency f (Hz) |
|---|---|---|
| 1 | 0,199 | 5,020 |
| 2 | 0,398 | 2,510 |
| **3** | **0,797** | **1,255** |
| 4 | 1,594 | 0,627 |
| 5 | 3,188 | 0,314 |
| 6 | 6,375 | 0,157 |
| 7 | 12,750 | 0,078 |
| 8 | 25,500 | 0,039 |
| 9 | 51,000 | 0,020 |
| 10 | 102,000 | 0,010 |
| 11 | 204,000 | 0,005 |

From the harmonics above, several different power spectra for the tower were simulated: Davenport, slightly modified Davenport, Harris and Kaimal. The Tables 9 and 10 show the *ck* coefficient results for the composition of fluctuating pressures for each power spectrum used.

Table 9. Decomposition of the fluctuating pressures (*ck*)

| k | ck - Davenport | ck – slightly modified Davenport | ck - Harris |
|---|---|---|---|
| 1 | 0,039320 | 0,039100 | 0,167838 |
| 2 | 0,065136 | 0,064772 | 0,182820 |
| 3 | 0,031199 | 0,031025 | 0,066596 |
| 4 | 0,094139 | 0,0963616 | 0,151900 |
| 5 | 0,098574 | 0,098039 | 0,105453 |
| 6 | 0,122335 | 0,121729 | 0,093217 |
| 7 | 0,145698 | 0,145219 | 0,080634 |
| 8 | 0,153372 | 0,153539 | 0,065151 |
| 9 | 0,126656 | 0,127649 | 0,045508 |
| 10 | 0,080190 | 0,081252 | 0,026753 |
| 11 | 0,043382 | 0,044059 | 0,014132 |

Table 10. Decomposition of the fluctuating pressures (*ck*) using the Kaimal spectrum

| k | ck (z=30m) | ck (z=24m) | ck (z=18m) | ck (z=12m) | ck (z=6m) |
|---|---|---|---|---|---|
| 1 | 0,032041 | 0,033157 | 0,034678 | 0,036932 | 0,040727 |
| 2 | 0,0529345 | 0,055751 | 0,057223 | 0,060873 | 0,066975 |
| 3 | 0,025285 | 0,026140 | 0,027300 | 0,029008 | 0,031842 |
| 4 | 0,075873 | 0,078357 | 0,081709 | 0,086600 | 0,094602 |
| 5 | 0,078478 | 0,080833 | 0,083966 | 0,088436 | 0,095461 |
| 6 | 0,096034 | 0,098464 | 0,101606 | 0,105894 | 0,112104 |
| 7 | 0,114496 | 0,116441 | 0,118780 | 0,121603 | 0,124760 |
| 8 | 0,130547 | 0,131026 | 0,131261 | 0,130832 | 0,128476 |
| 9 | 0,139014 | 0,136966 | 0,133915 | 0,129033 | 0,120447 |
| 10 | 0,135407 | 0,130573 | 0,124282 | 0,115643 | 0,102941 |
| 11 | 0,119890 | 0,113292 | 0,105281 | 0,095146 | 0,081666 |

The position of the gust center was considered at 24m above the ground to coincide with the top of module 2. Moreover, aiming to standardize the sensitivity analysis of the power density spectra in the Synthetic Wind Method, only one gust center situation was used. Based on the method's spatial correlation velocity, the Table 11 shows the fluctuating pressure reduction coefficient *Cr*. The distribution of the fluctuating wind pressure as well its gust center can be observed in Fig. 11.

Table 11. *Cr* values

| k | Gust size (m) | Cr for z=30 | Cr for z=24 | Cr for z=18 | Cr for z=12 | Cr for z= 6 |
|---|---|---|---|---|---|---|
| 1 | 1,07 | 0,000 | 1,000 | 0,000 | 0,000 | 0,000 |
| 2 | 2,14 | 0,000 | 1,000 | 0,000 | 0,000 | 0,000 |
| 3 | 4,28 | 0,000 | 1,000 | 0,000 | 0,000 | 0,000 |
| 4 | 8,55 | 0,299 | 1,000 | 0,299 | 0,000 | 0,000 |
| 5 | 17,11 | 0,649 | 1,000 | 0,649 | 0,299 | 0,000 |
| 6 | 34,22 | 0,825 | 1,000 | 0,825 | 0,649 | 0,474 |
| 7 | 68,43 | 0,912 | 1,000 | 0,912 | 0,825 | 0,737 |
| 8 | 136,86 | 0,956 | 1,000 | 0,956 | 0,912 | 0,868 |
| 9 | 273,73 | 0,978 | 1,000 | 0,978 | 0,956 | 0,934 |
| 10 | 547,46 | 0,989 | 1,000 | 0,989 | 0,978 | 0,967 |
| 11 | 1094,91 | 0,995 | 1,000 | 0,995 | 0,989 | 0,984 |

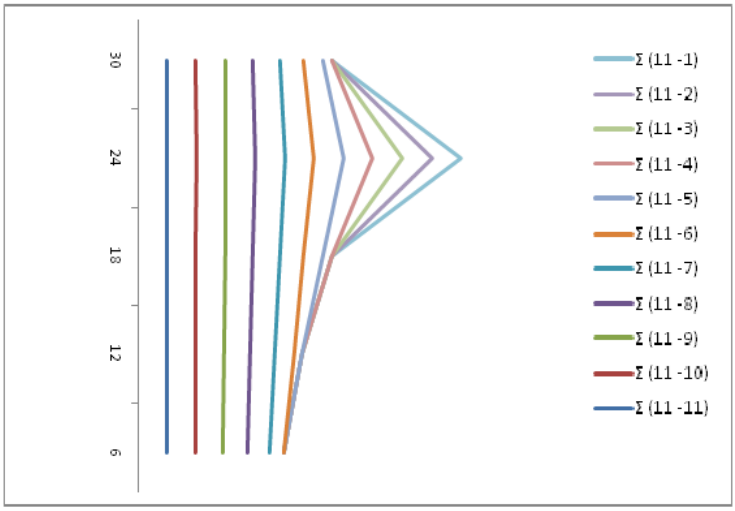


Figure 11. Fluctuating wind distribution and its gust center

## 5 Results and Conclusions

The displacement resulted from the analysis are from the three top nodes of the tower (nodes 46, 47 and 40, which are analogous to the nodes 1, 2 and 3 of the Fig. 10). The displacement for each the twenty combinations were statistically treated according to a Gaussian distribution with 95% probability of occurrence by:

$$u = \bar{u} + 1{,}65\sigma. \qquad (40)$$

where $u$ is the maximum probable displacement value, $\bar{u}$ is the displacement average and $\sigma$ the standard deviation.

The displacement results of the static part (equivalent to 48% of the total pressure) can be conferred at Table 12.

Table 12. Displacements of the static part

| 47: UY (m) | 46: UY (m) | 40: UY (m) |
|---|---|---|
| 0,22758 | 0,22758 | 0,22756 |

The displacements of the dynamic part for each spectrum used as well their statistical treatment can be seen in Table 13.

Table 13. Displacements of the dynamic part

| | Davenport | | slightly modified Davenport | | Harris | | Kaimal | |
|---|---|---|---|---|---|---|---|---|
| Case | UY 47 = 46 (m) | UY 40 (m) | UY 47 = 46 (m) | UY 40 (m) | UY 47 = 46 (m) | UY 40 (m) | UY 47 = 46 (m) | UY 40 (m) |
| 1 | 0,248774 | 0,248741 | 0,248352 | 0,248319 | 0,216091 | 0,216069 | 0,220723 | 0,220692 |
| 2 | 0,232771 | 0,232729 | 0,232869 | 0,232827 | 0,158266 | 0,158501 | 0,224160 | 0,224120 |
| 3 | 0,225363 | 0,225321 | 0,225324 | 0,225282 | 0,206376 | 0,206346 | 0,235642 | 0,235594 |
| 4 | 0,211086 | 0,211044 | 0,212042 | 0,212000 | 0,179137 | 0,179120 | 0,249594 | 0,249547 |
| 5 | 0,266738 | 0,266697 | 0,266441 | 0,266400 | 0,181776 | 0,181755 | 0,256555 | 0,256511 |
| 6 | 0,245512 | 0,245468 | 0,245609 | 0,277408 | 0,164933 | 0,164919 | 0,213782 | 0,213741 |
| 7 | 0,228385 | 0,228346 | 0,228757 | 0,228718 | 0,205498 | 0,205466 | 0,226703 | 0,226669 |
| 8 | 0,231421 | 0,231378 | 0,231005 | 0,230962 | 0,197080 | 0,197046 | 0,220849 | 0,220805 |
| 9 | 0,256320 | 0,256283 | 0,256866 | 0,256829 | 0,190864 | 0,190841 | 0,254720 | 0,254676 |
| 10 | 0,217245 | 0,217160 | 0,222038 | 0,222007 | 0,163450 | 0,163429 | 0,183449 | 0,183411 |
| 11 | 0,253165 | 0,253115 | 0,253967 | 0,253917 | 0,143128 | 0,144114 | 0,252684 | 0,252632 |
| 12 | 0,258245 | 0,258215 | 0,258109 | 0,258078 | 0,199177 | 0,199157 | 0,227876 | 0,227846 |
| 13 | 0,216729 | 0,216685 | 0,213957 | 0,213916 | 0,186668 | 0,186647 | 0,238375 | 0,238331 |
| 14 | 0,254059 | 0,254017 | 0,253860 | 0,253819 | 0,188604 | 0,186012 | 0,232871 | 0,232832 |
| 15 | 0,233515 | 0,233469 | 0,233869 | 0,233823 | 0,159586 | 0,159560 | 0,251351 | 0,251301 |
| 16 | 0,213558 | 0,213517 | 0,213618 | 0,213577 | 0,153279 | 0,153250 | 0,239247 | 0,239205 |
| 17 | 0,283374 | 0,283325 | 0,283127 | 0,283079 | 0,198705 | 0,198675 | 0,262586 | 0,261542 |
| 18 | 0,241752 | 0,241724 | 0,241530 | 0,241502 | 0,173671 | 0,173649 | 0,233557 | 0,233514 |
| 19 | 0,201236 | 0,201399 | 0,202579 | 0,202542 | 0,150833 | 0,150808 | 0,218328 | 0,218288 |
| 20 | 0,191394 | 0,191356 | 0,192048 | 0,192010 | 0,158274 | 0,158251 | 0,241246 | 0,241201 |
| $\bar{u}$ | 0,235532 | 0,235499 | 0,235798 | 0,237351 | 0,178770 | 0,178681 | 0,234215 | 0,234123 |
| $\sigma$ | 0,023232 | 0,023217 | 0,022940 | 0,024693 | 0,021391 | 0,021235 | 0,018493 | 0,018410 |
| u | 0,273864 | 0,273808 | 0,273649 | 0,278095 | 0,214066 | 0,213719 | 0,264728 | 0,264499 |

According to the Table 13, it is possible to notice that, among the evaluated power density spectra, the Original Davenport spectrum was the one that generated the largest statistically displacement response for nodes 46 and 47. The largest displacement response for the node 40 was obtained with the slightly modified Davenport spectrum. Due to the very similar formulation, the difference between the responses obtained with the original and modified Davenport spectrum was only 0,08% for nodes 46 and 47, and 1,54% for node 40. The Harris power spectral density proved to be the least conservative for this study, giving differences in relation to the largest dynamic displacement of 21,83% for nodes 46 and 47, and 23,15% for node 40. Such differences for the Kaimal spectrum were 3,34% for nodes 46 and 47, and 4,89% for node 40. Furthermore, it is noted that the results for the same spectrum between nodes 40, 46 and 47 are similar. Also, it is remarkable that the case that generated the largest displacement among the various spectra was the number 17, except for the Harris power spectrum, which had the largest displacement in the first combination.

The contrast between the response obtained with the Davenport and the Harris spectra is due to the difference between their scale lengths. However, it is not possible to state that the Kaimal spectrum in the Synthetic Wind Method results in more conservative values than the Harris power density spectrum. Therefore, to better evaluate the sensitivity of the Kaimal spectrum in the method it would be ideal to evaluate it with the other spectra in structures with various heights.

Moreover, a comparison of the displacement obtained by the static equivalent load analysis according to NBR 6123/1988 with the response obtained by the Synthetic Wind Method (SWM) was made (Table 14).

Table 14. Displacement difference between static and dynamic analysis with the Synthetic Wind Method with different power density spectra

| Method / Nodes | Displacement (m) | | Difference from the static analysis (%) | |
|---|---|---|---|---|
| | UY 47 = 46 | UY 40 | UY 47 = 46 | UY 40 |
| Static NBR 6123/1988 | 0,66310 | 0,66307 | - | - |
| SWM w/ Davenport | 0,50144 | 0,50139 | 24,38% | 24,38% |
| SWM w/ modified Davenport | 0,50123 | 0,50567 | 24,41% | 23,74% |
| SWM w/ Harris | 0,44165 | 0,44130 | 33,40% | 33,45% |
| SWM w/ Kaimal | 0,49231 | 0,49208 | 25,76% | 25,79% |

It is notable that the static analysis of the Brazilian standard resulted in the largest displacement at the top of the tower. Because the tower has a fundamental frequency greater than 1 Hz, it was already expected that the static analysis would give more conservative results than the dynamic analysis.

## Acknowledgements

Special thanks to the Brazilian research funding agency CAPES.

## References

[1] Brazilian National Standards Organization (Associação Brasileira de Normas Técnicas). *NBR 6123 – Building construction – Bases for design of structures – Wind loads – Procedure*, 1988.
[2] M. Franco. Direct along-wind dynamic analysis of tall structures. *Boletim técnico da Escola Politécnica da USP*, pp. 1-22, 1993.
[3] B. S. Taranath. *Structural analysis & design of tall buildings*. McGraw-Hill Inc., 1988.
[4] A. Nyberg and G. Söderlung. Wind-induced acceleration in high-rise building: An investigation on the dynamics effects due to a deep foundation. Master's Thesis, Chalmers University of Technology, 2017.
[5] R. A. Walley. Design techniques for practical wind problems. In: D. A, Howelles, I. P. Haigh and C. Taylos. *Dynamic waves in civil engineering*. Adlard & Son Ltd., pp. 57-67, 1971.
[6] J. Blessmann. *Introdução ao estudo das ações dinâmicas do vento.* Editora UFRGS, 2005.
[7] R. Magnago, G. Fisch and O. Moraes. Análise espectral do vento no centro de lançamento de Alcântra (CLA). *Revista Brasileira de Meteorologia*, 2010.
[8] R. M. L. R. F. Brasil and M. S. P. Silva. *Introdução à dinâmica das estruturas*. Blücher, 2013.
[9] A. G. Davenport. The spectrum of horizontal gustiness near the ground in high winds. *Quarterly Journal of the Royal Meteorological Society*, vol. 87, 1961.
[10] J. C. Kaimal, J. C. Wyngaard, Y. Izumi and O. R. Coté. Spectral characteristics of surface layer turbulence. *Quarterly Journal of the Royal Meteorological Society*, 1972.
[11] E. C. Lazanha. Análise dinâmica elasto-plástica de estruturas metálicas sob excitação aleatória do vento. Master's Thesis, Escola Politécnica da Universidade de São Paulo, 2003.
[12] H. A. Buchholdt and S. E. M. Nejad. *Structural Dynamics for Engineers*. ICE Publishing, 2012.
[13] E. B. Leite. Análise comparativa entre respostas de torre de transmissão sujeita a carregamentos obtidos através do método do vento sintético e da norma NBR 6123/88. Master's Thesis, Universidade Tecnológica Federal do Paraná, 2015.